RAPID COMMUNICATION

Microscale vortex laser with controlled topological charge*

Xing-Yuan Wang(王兴远)[1], Hua-Zhou Chen(陈华洲)[1], Ying Li(黎颖)[1], Bo Li(李波)[1], and Ren-Min Ma(马仁敏)[1,2,†]

[1] *State Key Laboratory for Mesoscopic Physics and School of Physics, Peking University, Beijing* 100871, *China*

[2] *Collaborative Innovation Center of Quantum Matter, Beijing, China*

(Received 20 October 2016; revised manuscript received 7 November 2016; published online 25 November 2016)

A microscale vortex laser is a new type of coherent light source with small footprint that can directly generate vector vortex beams. However, a microscale laser with controlled topological charge, which is crucial for virtually any of its application, is still unrevealed. Here we present a microscale vortex laser with controlled topological charge. The vortex laser eigenmode was synthesized in a metamaterial engineered non-Hermitian micro-ring cavity system at exceptional point. We also show that the vortex laser cavity can operate at exceptional point stably to lase under optical pumping. The microscale vortex laser with controlled topological charge can serve as a unique and general building block for next-generation photonic integrated circuits and coherent vortex beam sources. The method we used here can be employed to generate lasing eigenmode with other complex functionalities.

Keywords: exceptional point, non-Hermitian system, orbital angular momentum, vortex laser

PACS: 42.55.Px, 42.55.Sa, 42.60.By **DOI:** 10.1088/1674-1056/25/12/124211

1. Introduction

Vortex beams are light beams with helical phase front possessing infinite topological charge and a phase singularity at the beam axis.[1–3] These special properties inspired major interest for quantum information and communication, super-resolution imaging, micromanipulation, optical measurement, and digital imaging.[4–14] The generation of optical vortex beam relies on the phase modulation of a laser beam either inside or outside of a laser cavity.[1–3,15–29] To miniaturize the vortex beam generator, Cai *et al*. demonstrated an on-chip vortex emitter with well-defined orbital angular momentum by coupling light into a micro-ring with azimuthal scattering gratings.[30] Recently, researches on metamaterial and exceptional point have provided a general method to manipulate electromagnetic field in a controlled manner.[31–42] Miao *et al*. demonstrated a laser with emission carrying orbital angular momentum at microscale.[43] However, a microscale laser with controlled topological charge, which is crucial for virtually any of its application, is still unrevealed.

Here we demonstrated avortex laser with controlled topological charge at microscale. The vortex laser eigenmode synthesized in a micro-ring cavity at the exceptional point is stable enough to lasing state and emits vortex beam directly under optical pumping. Such a system can generate different orders of vortex beams by simply modulatingthe grating protruded on the micro-ring cavity. We obtained all these results from rigorous theoretical derivation and further proved them using three-dimensional (3D) full wave simulations.

2. Methods

2.1. Theoretical derivation

As for the vortex laser design, the key point is to construct an eigenmode in the microcavity which can emit vortex beam at desired order. First of all, we presented an analytical analysis for all kinds of exceptional points in a micro-ring cavity in the parameter space. Exceptional point is a singularity where both eigen-frequency and eigen-function coalesce. Here we employed a general form of refractive index modulation along the azimuthal direction of a micro-ring cavity and derived the conditions of exceptional point based on the coupled mode theory. Then, from the physical picture of scattering waves interference, we obtained the equations describing the parameters relationships of the refractive index modulations to achieve the exceptional point where only one propagating whispering-gallery mode exist at the lasing frequency. Secondly, a non-zero momentum perpendicular to the micro-ring plane is generated by introducing periodic gratings on the out wall of the micro-ring cavity. The out-of-plane momentum and the micro-ring cavity eigen-mode will twisted into an optical vortex beam. we can tune the order of the optical vortex emission by simply tuning the number of the grating elements along the outer sidewall.

2.2. Numerical simulation

The characteristics of the vortex laser is analyzed by 3D full wave simulations (Comsol Multiphysics). For a vortex

*Project supported by the "Youth 1000 Talent Plan" Fund, Ministry of Education of China (Grant No. 201421) and the National Natural Science Foundation of China (Grant Nos. 11574012 and 61521004).

†Corresponding author. E-mail: renminma@pku.edu.cn

© 2016 Chinese Physical Society and IOP Publishing Ltd

laser cavity based on III–V InGaAsP gain materials as an example, the three dimensional eigen-mode solution will give all the information of the field distribution. The pumping effect of the cavity is treated as an increase of the imaginary part of InGaAsP refractive index. The stability of the vortex laser during the pumping is verified by the chirality of the angular momentum distribution in the lasing process. Q factor is calculated by the formula $Q = f_r/2f_i$, where f_r and f_i are the real and imaginary part of the eigenfrequency. Details forspecific parameters can be found in the corresponding figure captions.

3. Results and discussion

3.1. Principles of a vortex laser

Figure 1 is the schematic diagram of a vortex laser. This vortex laser can generate arbitrary order of vortex beam. Here, we choose the second-order vortex beam as an example. Figure 1(a) presents the perspective view of the magnetic field $|H|$ distribution of a full wave simulation of the vortex laser on a log scale. Inside the laser cavity, the exceptional point ensures a unidirectional travelling whispering gallery mode, which is evidenced by the weak fluctuation of the magnetic field (Fig. 1(b)). Figure 1(c) shows the transversal distribution of the radial component of the magnetic field H_r in the far field, which presents a vortex beam profile. The vortex laser cavity is simulated with III–V InGaAsP gain materials, because its emission is at the C-band of the optical communication.[44] The inner radius and the width of the vortex laser cavity are 1500 nm and 500 nm respectively.

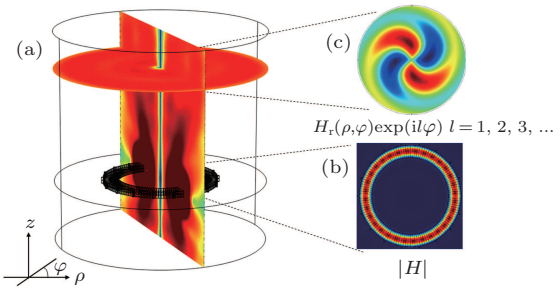


Fig. 1. (color online) Operation principles of a vortex laser. (a) A perspective view of the magnetic field $|H|$ distribution of a full wave simulated vortex laser on a log scale. (b) The exceptional point enables a unidirectional travelling whispering gallery mode inside the laser cavity evidenced by the weak fluctuation of magnetic field $|H|$. (c) The transversal distributions of radial component of the magnetic field H_r in the cross section of the vortex laser emission, showing typical optical vortex beam characteristic.

3.2. Exceptional points in the vortex laser cavity

The chirality mode at exceptional point is necessary for the realization of vortex laser with well-defined topological charge. Here we derived a general expression for the exceptional points in a vortex laser cavity. The derivation is based on the unsymmetrical coherent scattering between two degenerate counter propagating modes in a whispering-gallery micro-ring cavity. In a fundamental physical picture of interference, when the back scatterings from counter-clockwise (CCW) mode to clockwise (CW) mode interfere destructively while the back scatterings from CW mode to CCW mode do not, the system locates at the exceptional point and degenerate eigen-modes of the system coalesce to a pure CCW traveling mode and *vice versa*.[40] Here we employed two sets of periodic gratings to generate discrete momentums satisfying the resonance Bragg-scattering condition. Figure 2(a) shows a general form of the refractive index modulation along the azimuthal direction (φ):

$$n = \begin{cases} n_0 + \Delta_1 \mathrm{e}^{\mathrm{i}\phi_1}, & (l\pi/m \le \varphi \le l\pi/m + \delta\varphi_1), \\ n_0 + \Delta_2 \mathrm{e}^{\mathrm{i}\phi_2}, & (l\pi/m + \varphi_0 \le \varphi \le l\pi/m + \varphi_0 + \delta\varphi_2), \end{cases} \quad (1)$$

where $l = 0, 1, 2, \ldots, 2m-1$. The micro-ring is divided into $2m$ periods. n_0 is the unperturbed part of the refractive index. The index modulation is given by complex number $\Delta_2 \mathrm{e}^{\mathrm{i}\phi_2}$ and $\Delta_1 \mathrm{e}^{\mathrm{i}\phi_1}$.

The two gratings, $\Delta n = \Delta_1 \mathrm{e}^{\mathrm{i}\phi_1}$ and $\Delta n = \Delta_2 \mathrm{e}^{\mathrm{i}\phi_2}$ can be viewed as two sources of scattering. The modulus of the effective refractive index modulation induced by each grating will modulate the amplitude of the corresponding backscattering while its position and the angular width of the effective refractive index modulation (ϕ_1 and ϕ_2) decides the relative phase of the corresponding back scattering. Based on the mode coupling theory, we can obtain all the possible grating configurations to achieve fully destructive interference in one direction with nondestructive interference in the other direction, *a.k.a.* the exceptional point in the vortex laser cavity.

Here, we show two special classes of exceptional points with simplified parameters: 1) $\delta\varphi_1 = \delta\varphi_2$, 2) $\phi_1 = 0$, and 3) $\phi_2 = \pi/2$, where parity time symmetry is included in both cases.

In case 1), where the two modulation parts have the same angular width $\delta\varphi_1 = \delta\varphi_2$, the refractive index modulation to realize exceptional points needs to satisfy the relations of $\Delta_1 = \Delta_2$ and $\phi_2 + 2m\varphi_0 - \phi_1 = \pi$. $\delta\varphi_1 = \delta\varphi_2$ and $\Delta_1 = \Delta_2$ ensure equal amplitudes of back scatterings. The initial phase difference of the two back scatterings is $\phi_2 - \phi_1$. The angular displacement φ_0 between the centers of the two gratings provides additional phase difference of $2m\varphi_0$. The two back scatterings interfere destructively when the total phase difference $\phi_2 + 2m\varphi_0 - \phi_1$ equals to π, leading to an exceptional point for the unidirectional traveling CCW mode.

Another class of refractive index modulation is case 2) $\phi_1 = 0$ and $\phi_2 = \pi/2$. Figures 2(b) and 2(c) show the relations the parameters need to satisfy. The systems with parameters locating at the parameter surface in Figs. 2(b) and 2(c) are at certain exceptional point. We can see that the PT-symmetrical refractive index modulation is only a special case ($2m\varphi_0 = \pi/2$, $2m\delta\varphi_1 = 2m\delta\varphi_1 = \pi$, and $\Delta_1 = \Delta_2$). To illustrate this, we solved the eigen-value problem under the condition of $\phi_1 = 0, \phi_1 = \pi/2$, $2m\varphi_0 = \pi/2$. Figures 2(d) and 2(e) show the real part and imaginary part of the eigen-values respectively. Obviously, the systems corresponding to the clinodiagonal of the $n_R - n_I$ coordinate plate ($\Delta_1 = \Delta_2$) have coalesced eigen-value and thus locate at exceptional point.

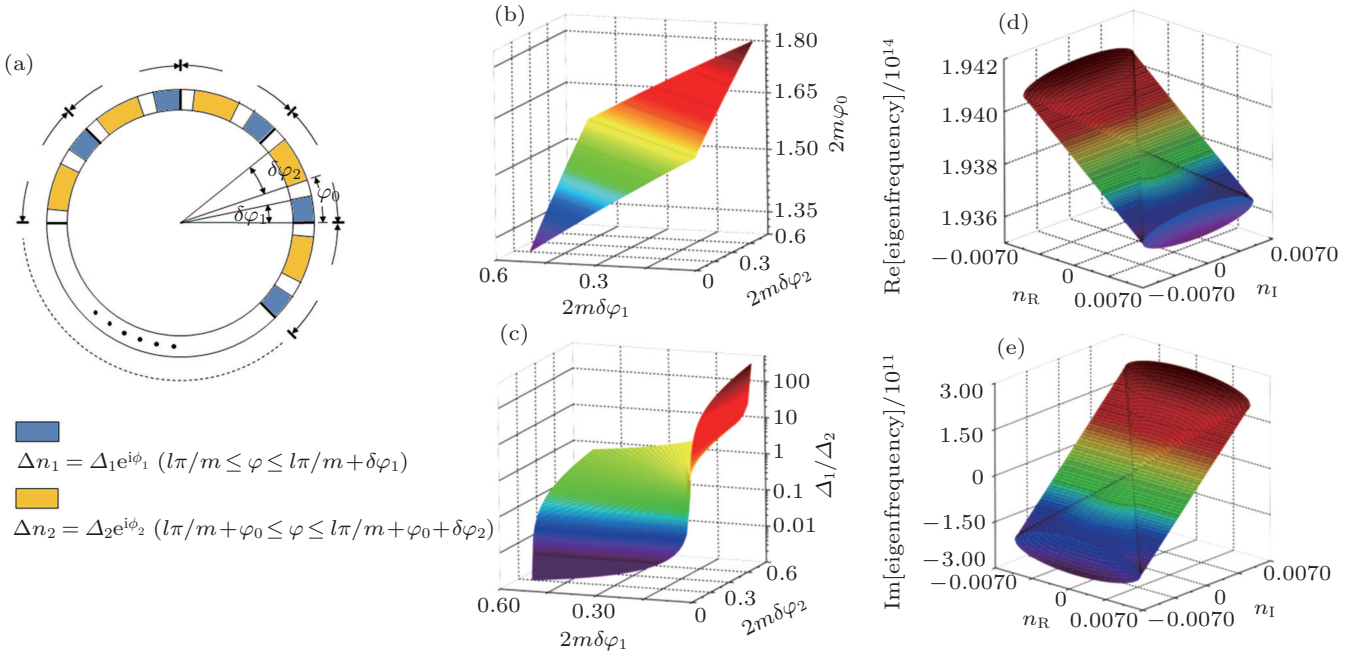


Fig. 2. (color online) Exceptional points in the vortex laser cavity. (a) A general form of refractive-index modulation in a micro-ring cavity. The index modulation consists of two sets of periodic scattering elements, which are essential to realize exceptional points in the view of interference. Panels (b) and (c) show the relations the parameters need to satisfy simultaneously to achieve exceptional points on the condition of $\phi_1 = 0$ and $\phi_2 = \pi/2$. Panels (d) and (e) are the real part and imaginary part of the eigen-values in the case of one grating with pure real part n_R ($n_R = \Delta_1 e^{i\phi_1}, \phi_1 = 0$) while the other grating with pure imaginary n_I ($n_I = \Delta_2 e^{i\phi_2}$, $\phi_2 = \pi/2$) index modulation and keeping $2m\varphi_0 = \pi/2$. This is the case of PT-symmetrical refractive index modulation. In the calculation, azimuthal order $m = 16$, refractive index of the cavity $n_0 = 2.67$, $\Delta n_R = n\pi/16 \le \varphi \le n\pi/16+\pi/32$, $\Delta n_I = n\pi/16+\pi/64 \le \varphi \le n\pi/16+3\pi/64$, $n = 0, 1, 2, \ldots, 31$. The inner radius and the width of the vortex laser cavity is 1500 nm and 500 nm respectively.

3.3. Different orders of optical vortex generation on demand

Optical vortex with different orders of orbital angular momentum has an additional degree of freedom for multiplexing. Here, we presented the generation of optical vortex with different order while in the PT-symmetrical refractive index modulated system:

$$n = \begin{cases} n_0+\Delta n_R, & (l\pi/m \le \varphi \le l\pi/m+\pi/4m), \\ n_0+\Delta n_R+\Delta n_I i, & (l\pi/m+\pi/4m \le \varphi \le l\pi/m+\pi/2m), \\ n_0+\Delta n_I i, & (l\pi/m+\pi/2m \le \varphi \le l\pi/m+3\pi/4m), \end{cases} \tag{2}$$

where n_0 is the unperturbed part of the refractive index, and Δn_R and Δn_I are the real and imaginary index modulation, respectively. $l = 0, 1, 2, \ldots, 2m-1$.

The $2m$ periods of refractive index modulation is chosen to tune the system to an exceptional point. At the same time the index modulation will not couple the beam into free space according to momentum-matching condition. This ensures that we can avoid uncontrollable additional orders of vortex beam. And then we choose the number of the outer sidewall grating q_{OWG} as $2m > q_{OWG} > m$. In this case, the outer sidewall grating does not cause the change of the exceptional point in parameter space. It only takes the role of coupling the travelling whispering-gallery mode and the free-space vortex beam mode. The order ν_{rad} of the optical vortex is solely determined by the difference between azimuthal order m of the desired whispering gallery mode and the number of the outer sidewall gratings:

$$\nu_{rad} = m - q_{OWG}. \tag{3}$$

The general results obtained are valid for both TE and TM polarized whispering-gallery modes. In our device with thin ring geometry, the effective index for TM modes is considerably decreased.[45] Thus, the TE modes preferentially reach the lasing condition of the cavity. The magnetic field vector H_z of the TE modes are perpendicular to the cavity plane.

Vortex beams with arbitrary orbital angular momentum can be achieved by tuning the outer sidewall grating. Figure 3 shows that stable vortex beam with increasing orbital angular momentum can be obtained by changing q_{OWG}. As shown in Figs. 3(a), 3(e), and 3(i), almost homogeneous magnetic field intensity distributions on the ring can be obtained for generating different orders of optical vortex. The fluctuation of the corresponding field intensity distribution $|H|$ in the cross sec-

tion of the vortex beam is also very weak (Figs. 3(b), 3(f), and 3(j)). The transversal distributions of radial component H_r (Figs. 3(c), 3(g), and 3(k)) and the corresponding phase distributions arg (H_r) (Figs. 3(d), 3(h), and 3(l)) further confirm that the vortex beams emitted from cavities with outer sidewall grating elements $q_{OWG} = 17, 18, 19$ have definite OAM $\hbar$, $2\hbar$, and $3\hbar$, respectively, which can be calculated from Eq. (3). These results are direct evidences indicating that the vortex laser can generate optical vortex with controllable definite orbital angular momentum.

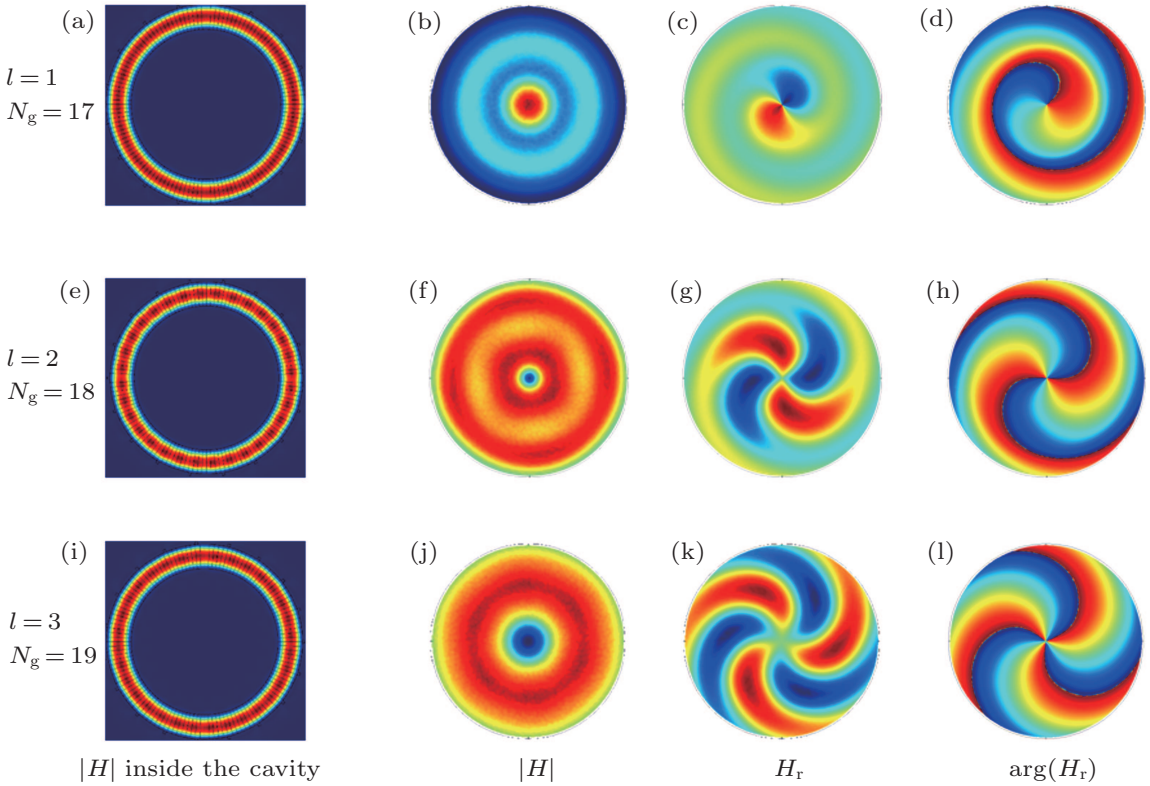


Fig. 3. (color online) Different orders of optical vortex generation on demand. (a)–(d) A Vortex laser with the first order of orbital angular momentum optical vortex emission, where the magnetic field intensity distributions inside the laser cavity (a), and $|H|$ (b), H_r (c), and arg (H_r) (d) at 4 μm above the lase cavity are depicted. (e)–(h) A Vortex laser with the second order of orbital angular momentum optical vortex emission, where the magnetic field intensity distributions inside the laser cavity (e), and $|H|$ (f), H_r (g), and arg (H_r) (h) at 4 μm above the lase cavity are depicted. (i)–(l) A Vortex laser with the third order of orbital angular momentum optical vortex emission, where the magnetic field intensity distributions inside the laser cavity (i), and $|H|$ (j), H_r (k), and arg (H_r) (l) at 4 μm above the lase cavity are depicted. All systems have the same index modulation ($\Delta n_R = \Delta n_I = 0.01$).

3.4. Visualization of vortex laser orbital angular momentum distribution

To further confirm the generation of the specific order of optical vortex, we decomposed the light field in the far field into a series of eigen-modes with different orbital angular momentum while the principle of the realization of vortex mode is also clearly shown. The field distribution can be decomposed by being expanded in cylindrical harmonics,[45,46]

$$H_z(r,\varphi) = \sum_{m=-\infty}^{\infty} \alpha_m \mathrm{J}_m(nkr)\exp(\mathrm{i}m\varphi), \tag{4}$$

where J_m is the m-th order Bessel function of the first kind, and k is the wave number, and n is the effective refractive index of the micro-ring. The CW (CCW) traveling-wave components are denoted by positive (negative) values of the angular momentum index m.[46]

Figures 4(a) and 4(b) show the simulated intensity patterns $|H|$ and H_z in the far field of a vortex laser cavity for generation of second order of orbital angular momentum emission. We can see that the fluctuation of the simulated magnetic pattern $|H|$ (Fig. 4(a)) is negligible at exceptional point. Figure 4(c) shows the ratio of the CW and CCW components $|\alpha_m|^2/|\alpha_{-m}|^2$ as a function of real index modulation Δn_R with fixed $\Delta n_I = 0.01$. The exceptional point locates at $\Delta n_R = \Delta n_I$, at which the real and imaginary parts of the eigen-frequencies coalesce simultaneously. At $\Delta n_R = 0$, both eigenmodes have equal CW and CCW components $\left(|\alpha_{16}|^2/|\alpha_{-16}|^2 \sim 1\right)$ while in the vicinity of the exceptional point ($\Delta n_R = \Delta n_I$), both eigenmodes have dominant CCW component $\left(|\alpha_{16}|^2/|\alpha_{-16}|^2 \gg 1\right)$. These show an evolution from standing waves to traveling wave when the system is approaching the exceptional point. Especially, the simulation shows that the CCW component is about 484 times larger than the CW component at exceptional point, indicating a nearly perfect traveling wave mode.

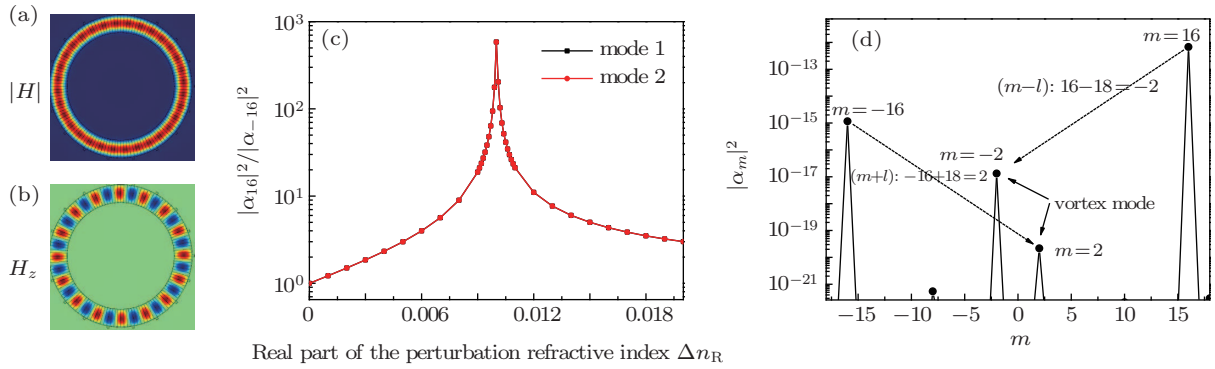


Fig. 4. (color online) Visualization of vortex laser angular momentum distribution. Panels (a) and (b) show the simulated intensity patterns $|H|$ and H_z of a mode inside the vortex laser cavity at $\Delta n_R = \Delta n_I$. The weak fluctuation of the $|H|$ and the periodicity of the H_z clearly show a 16-order traveling mode. (c) Ratio of CW and CCW component $|\alpha_m|^2/|\alpha_{-m}|^2$ as a function of real index modulation Δn_R. The imaginary index modulation is fixed at $\Delta n_I = 0.01$. The mode shows clear chirality in the vicinity of the exceptional point ($\Delta n_R = \Delta n_I$). The CCW component is about 484 times larger than the CW component at exceptional point, which indicates a nearly perfect traveling wave mode. (d) Angular momentum distribution $|\alpha_m|^2$ of the whispering-gallery mode at exceptional point ($\Delta n_R = \Delta n_I = 0.01$). The outer sidewall grating elements ($q_{OWG} = 18$) couple the dominated CW mode to the vertically emitted vortex beams with orbital angular momentum index $m = -2$ (16–18).

Figure 4(d) shows the orbital angular momentum distribution of the mode at exceptional point, which illustrates the physical process of the creation of the vortex beam. Under the index modulation, the CW modes are dominant (two orders larger than the CCW component while $m = 16$), and the outer sidewall grating elements ($q_{OWG} = 18$) couples CW and CCW traveling modes to the vertically emitting vortex beams with orbital angular momentum indexes $m = -2$ and $m = 2$, respectively. Thus, the emitted vortex beam with $m = -2$ from CW mode is two orders larger than the vortex beam with $m = 2$ from CCW mode, generating a vortex beam with definite angular momentum.

3.5. Stability of the vortex-beam output in the lasing process under pumping

Exceptional point is sensitive to the environmental parameters. Here we illustrate the stability of the vortex laser in the lasing process under uniform pumping. The uniform pumping of the gain material InGaAsP of the cavity is equivalent to increasing the imaginary part of refractive index n_I of the InGaAsP. The uniformly changed background refractive index n_I will only cause the change of the first order of the Fourier expansion coefficient of the refractive index, which will not induce additional coupling between the CCW and CW whispering-gallery modes according to the phase matching condition, and thus will not cause the change of the exceptional point in parameter space. We have confirmed this by 3D full wave simulations. As shown in Fig. 5(a), the vortex laser cavity mode becomes lasing and emitting vortex beam with the increase of n_I. However, the ratio of orbital angular momentum components is almost unchanged as shown in Fig. 5(b), which confirms that the vortex laser is stable in the lasing process. The system is stable while $n_I = -0.005$, corresponding to material gain of 202.5 cm^{-1}, which is achievable in InGaAsP system.[47]

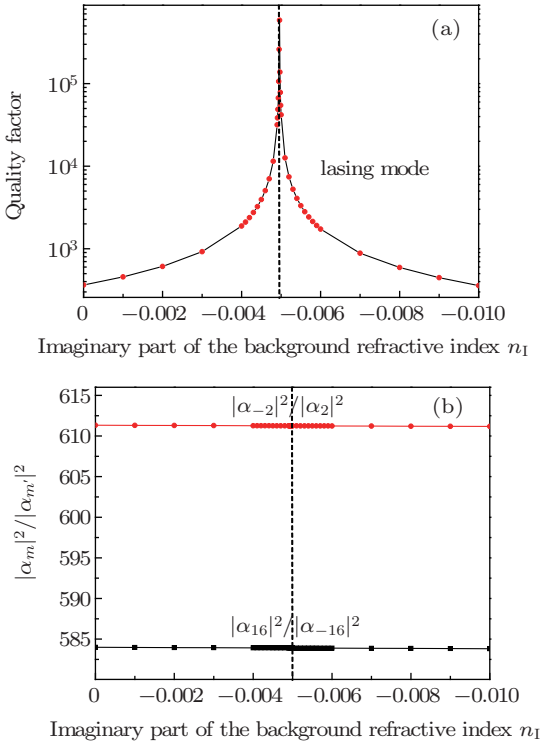


Fig. 5. (color online) Stability of the vortex-beam output in the lasing process under pumping. (a) The background gain dependence of the cavity quality factor for a vortex beam laser at exceptional point ($\Delta n_R = \Delta n_I = 0.01$) with $N_g = 19$. The uniform pumping gain of the InGaAsP ring is mimicked by increasing the imaginary part of background refractive index n_I. The quality factor is about 365 for the cavity without gain. With the increasing of the gain coefficiency, the cavity quality factor increases by orders of magnitude, indicating that the loss is compensated by the gain. (b) Ratio of the CW and CCW components $|\alpha_m|^2/|\alpha_{-m}|^2$ as a function of background refractive index n_I. The black dots show the main component of the mode is CW mode, which is almost unchanged with the increase of the background refractive index n_I. The CW traveling mode is coupled to a vortex beam with azimuthal quantum number $m = -2$ (see the red dots).

4. Conclusions

In conclusion, the microscale vortex laser with controlled topological charge is demonstrated. The vortex laser eigen-

mode was synthesized in a meta-materials engineered non-Hermitian micro-ring cavity system and the optical vortex emission with defined orbital angular momentum can be obtained in a controlled manner. The vortex laser with controlled topological charge synergizes lasing and modulating functionalities in one device with microscale footprint, making it a unique and general building block for next-generation photonic integrated circuits and coherent vortex beam source.

References

[1] Padgett M, Courtial J and Allen L 2004 *Phys. Today* **57** 35
[2] Allen L, Beijersbergen M W, Spreeuw R and Woerdman J P 1992 *Phys. Rev. A* **45** 8185
[3] Yao A M and Padgett M J 2011 *Adv. Opt. Photon.* **3** 161
[4] Mair A, Vaziri A, Weihs G and Zeilinger A 2011 *Nature* **412** 313
[5] Molina-Terriza G, Torres J P and Torner L 2007 *Nat. Phys.* **3** 305
[6] Wang J, Yang J Y, Fazal I M, *et al*. 2012 *Nat. Photon.* **6** 488
[7] Hui X N, Zheng S L, Chen Y L, *et al*. 2015 *Sci. Rep.* **5** 10148
[8] Tamburini F, Anzolin G, Umbriaco G, Bianchini A and Barbieri C 2006 *Phys. Rev. Lett.* **97** 163903
[9] He H, Heckenberg N R and Rubinszteindunlop H 1995 *J. Mod. Opt.* **42** 217
[10] Friese M, Enger J, Rubinszteindunlop H and Heckenberg N R 1996 *Phys. Rev. A* **54** 1593
[11] Toyoda K, Miyamoto K, Aoki N, Morita R and Omatsu T 2012 *Nano Lett.* **12** 3645
[12] Zhou Z Y, Li Y, Ding D S, *et al*. 2014 *Opt. Lett.* **39** 5098
[13] Fürhapter S, Jesacher A, Bernet S and Ritsch-Marte M 2005 *Opt. Lett.* **30** 1953
[14] Torner L, Torres J P and Carrasco S 2005 *Opt. Express* **13** 873
[15] Beijersbergen M W, Coerwinkel R, Kristensen M and Woerdman J P 1994 *Opt. Commun.* **112** 321
[16] Li H L, Phillips D B, Wang X Y, *et al*. 2015 *Optica* **2** 547
[17] Heckenberg N R, Mcduff R, Smith C P and White A G 1992 *Opt. Lett.* **17** 221
[18] Marrucci L, Manzo C and Paparo D 2006 *Phys. Rev. Lett.* **96** 163905
[19] Yu N F, Genevet P, Kats M A, *et al*. 2011 *Science* **334** 333
[20] He J W, Wang X K, Hu D, *et al*. 2013 *Opt. Express* **21** 20230
[21] Senatsky Y, Bisson JF, Li J, Shirakawa A, Thirugnanasambandam M and Ueda K I 2012 *Opt. Rev.* **19** 201
[22] Oron R, Davidson N, Friesem A A, Hasman E and 2000 *Opt. Commun.* **182** 205
[23] Oron R, Danziger Y, Davidson N, Friesem A A and Hasman E 1999 *Opt. Commun.* **169** 115
[24] Bisson J F, Senatsky Y and Ueda K I 2005 *Laser Phys. Lett.* **7** 327
[25] Itoh M and Yatagai T 2005 *Opt. Express* **15** 7616
[26] Caley A J, Thomson M J, Liu J S, Waddie A J and Taghizadeh M R 2007 *Opt. Express* **15** 10699
[27] Ito A, Kozawa Y and Sato S 2010 *J. Opt. Soc. Am. A* **27** 2072
[28] Kano K, Kozawa Y and Sato S 2012 *Int. J. Opt.* **359** 141
[29] Naidoo D, Roux F S, Dudley A, *et al*. 2016 *Nat. Photon.* **10** 327
[30] Cai X L, Wang J W, Strain M J, *et al*. 2012 *Science* **338** 363
[31] Heiss W D 2004 *J. Phys. A: Math. Gen.* **37** 2455
[32] Wiersig J 2014 *Phys. Rev. A* **89** 012119
[33] Lin Z, Ramezani H, Eichelkraut T, *et al*. 2011 *Phys. Rev. Lett.* **106** 213901
[34] Peng B, Ozdemir S K, Rotter S, *et al*. 2016 *Porc. Natl. Acad. Sci.* **113** 6845
[35] Liertzer M, Ge L, Cerjan A, *et al*. 2012 *Phys. Rev. Lett.* **108** 173901
[36] Peng B, Ozdemir S K, Rotter S, *et al*. 2014 *Science* **346** 328
[37] Dembowski C, Graf H D, Harney H L, *et al*. 2001 *Phys. Rev. Lett.* **86** 787
[38] Heiss W D and Harney H L 2001 *Eur. Phys. J. D* **17** 149
[39] Cao H and Wiersig J 2015 *Rev. Mod. Phys.* **87** 61
[40] Zhu J G, Ozdemir S K, He L N and Yang L 2010 *Opt. Express* **18** 23535
[41] Wiersig J 2014 *Phys. Rev. Lett.* **112** 203901
[42] Wiersig J 2016 *Phys. Rev. A* **93** 033809
[43] Miao P, Zhang Z, Sun J, *et al*. 2016 *Science* **353** 464
[44] Killinger D 2002 *Opt. Photon. News* **13** 36
[45] Frateschi N C and Levi A F J 1996 *J. Appl. Phys.* **80** 644
[46] Wiersig J, Eberspacher A, Shim J B, *et al*. 2011 *Phys. Rev. A* **84** 023845
[47] Leuthold J, Mayer M, Eckner J, Guekos G and Melchior H 2000 *J. Appl. Phys.* **87** 618